

HYPERFINE STRUCTURE ON CYLINDRICAL FRESNEL LENSES FOR HOLOGRAPHIC LABELS

Mona MIHĂILESCU¹, Eugen SCARLAT², Augusta Raluca GABOR³, George BOSTAN⁴, Vlad MELU⁴

An ensemble of cylindrical Fresnel lenses designed to exhibit the same focal length at three distinct wavelengths is presented. To control the lateral displacement of focal lines in millimeter range, hyperfine rectilinear gratings are superposed on each lens. The ensemble is designed as security elements to be integrated on holographic labels. Simulations as well as experimental results are presented. Before manufacturing the microrelief on transparent polymers, a dynamic mechanical analysis was performed. The geometrical characterization of the microrelief was undertaken by the help of quantitative phase imaging.

Keywords: cylindrical Fresnel lens, hyperfine grating, foci control, diffracted intensity pattern, holographic label, security element.

1. Introduction

The standard concept of the holographic label consists of an aluminum foil with printed microrelief which diffracts the incident white light, giving rise to optical images with multiple effects. The more complex the optical effects or hidden elements, the more secure holographic mark. Consequently, a dense spatial packing of the diffractive microreliefs at the best spatial resolution are essential when imprinting the details.

Diffractive optics design allows the superposition of structures with already proved usefulness: circular and rectilinear diffraction gratings arrangements [1], rectilinear gratings at various angles [2], and with different constants for Talbot interferometer [3], or for controlling the field absorption in the case of solar cells [4]. Diffractive structures with cylindrical symmetry demonstrated their functionality as spectrum splitters [5]. To generate twin focal points, diffractive microstructures with asymmetric geometry based on Fresnel lenses were used [6].

¹ Prof. Dept. of Physics, Research Centre for Fundamental Sciences Applied in Engineering, National University for Science and Technology POLITEHNICA Bucharest, Romania, e-mail: mona.mihaiescu@upb.ro

² Dept. of Physics, National University for Science and Technology POLITEHNICA Bucharest, Romania, e-mail: eugen.scarlat@upb.ro

³ Eng., National Institute for Research in Chemistry, Romania, e-mail: raluca.gabor@icechim.ro

⁴ Eng., S. C. Optoelectronica 2001 S.A., Romania, e-mail: george@optoel.ro

To enhance the security level of the holographic labels here we propose an ensemble of cylindrical Fresnel lenses (CFL) with spatially controlled focal positions for three distinct wavelengths. A hyperfine rectilinear grating with adaptive period is superposed onto the lenses configuration to introduce steering and focusing effects at distinct wavelengths and at controlled distances in planes perpendicular to the propagation axis. Technically, the holographic mark carrying the CFL ensemble appears as a classical barcode to the naked eyes, but it reveals the rectilinear foci distribution only when illuminated with the proper wavelengths of a tunable He-Ne laser, i.e., 543nm, 594nm, and 633nm. Therefore, the CFL ensemble is a hidden security element that cannot be seen with the naked eye in white light but only with the help of adequate instruments like lasers of precise wavelengths.

2. Diffractive structures design

To be consistent with the available manufacturing technology, the CFL ensemble was designed as a phase only device with two phase levels which correspond to two step microrelief in the fabrication process. To obtain cylindrical symmetry, first we designed circular Fresnel lenses characterized by geometrical parameters (zone index a , and zone radius r_a) in relation with the optical parameters (the focal length f , and the wavelength λ) [7]:

$$r_a^2 = 2 \cdot f \cdot a \cdot \lambda \quad (1)$$

The equation was implemented in MATLAB as 1920×1200 matrix with binary values. Second, the diameter line of the circular lens was extracted to generate the CFL by replicating it along a convenient distance, i.e., equal with the width of the laser beam used to illuminate it. CFL is characterized by the reflection function $R(x,y)$ which focuses the radiation as a bright sharp line at precise distance along the propagation direction.

We designed a hybrid CFL consisting of the concatenation of three CFLs (Fig.1a) with the corresponding hyperfine rectilinear structures (Fig.1b). The concatenation means the side-gluing the fractions of CFLs, keeping for each the central portion (the widest black areas) and as much as possible from the adjacent areas.

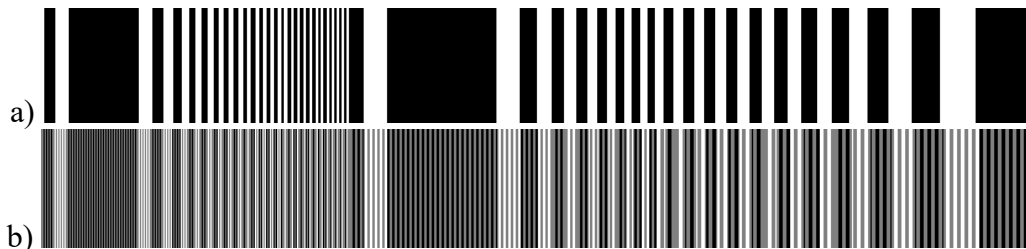


Fig.1. Cylindrical Fresnel lens: a) without hyperfine structure, b) with hyperfine structure

In the absence of the hyperfine gratings, each CFL is designed to exhibit the same focal length at the specific wavelength it operates (543nm, 594nm, or 633nm), so the foci would be very close each other in any transversal plane along the propagation direction. The grating introduces the wavelength dependent, lateral displacement of the line-shaped foci and avoids their overlapping. Fig.2 illustrates the lateral spread of the focal lines in a plane perpendicular to the propagation axis.

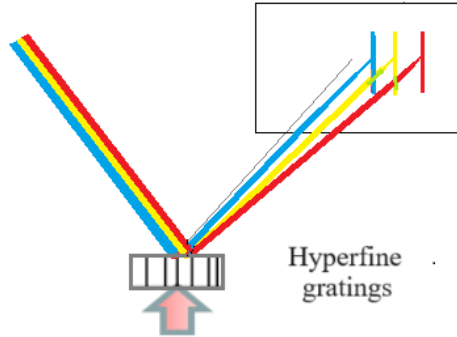


Fig 2. Foci lateral displacements due to the hyperfine gratings

3. Propagation simulation

The light propagation through CFL ensemble was simulated in MATLAB using scalar diffraction theory in Fresnel approximation. As input parameters, we considered a monochromatic wavelength λ , normally incident on CFL characterized by the reflectance function $R(x,y)$ situated at $z=0$ (the input plane). $R(x,y)$ is considered a binary diffractive element and corresponds to the phase mask of the diffractive CFLs.

At the distance z from the CFL, the complex diffracted field $U(x_z, y_z, z)$ can be expressed using the 2-D convolution involving CFL reflectance [8]:

$$U(x_z, y_z, z) = R(x, y, 0) \otimes h(x, y, x_z, y_z, z) \quad (2)$$

where

$$h(x, y, x_z, y_z, z) = \frac{\exp(ik \cdot s_{01})}{i\lambda \cdot s_{01}} \quad (3)$$

stands for the impulse response function, (x, y) are the coordinates in the input plane (CFL plane), and (x_z, y_z) are the coordinates in the diffracted intensity plane, situated at distance z ; s_{01} is the distance between any two points from the input plane and the output plane, whilst $k = 2\pi / \lambda$ is the wavenumber. Eq.(2) is formally converting the distribution of the input field into the output diffracted intensity pattern. The implementation of Eq.(2) and the simulation procedures (Nyquist spatial sampling, MATLAB developed scripts, the relationships between the spatial variables and the pixel dimensions, etc.) are largely described in [9].

In Fig.3 a-c are shown the simulated diffracted beams focused on a screen perpendicular to the propagation axis for each CFL at designed wavelength if it would be alone. Since the laser beam cross sectional area is large enough to cover all concatenated CFLs, it follows for each wavelength there are three foci at different distances, one for each individual CFL. Consequently, there are three distances where a part of the beam is clearly focused, the other parts appearing as two thick, less intense, blurred profiles (Fig.3d). By denoting f_{ij} the focal length of the CFL r_j when illuminated by the wavelength λ_j , $i,j=1,2,3$, and the designed, common focal distance $f=f_{ii}$, one gets the relationships among the focal distances by applying Eq.(1):

$$f_{ij} = f \cdot \frac{\lambda_i}{\lambda_j} \quad (4)$$

$$\frac{f_{ij}}{f_{ji}} = \frac{\lambda_i^2}{\lambda_j^2} \quad (4')$$

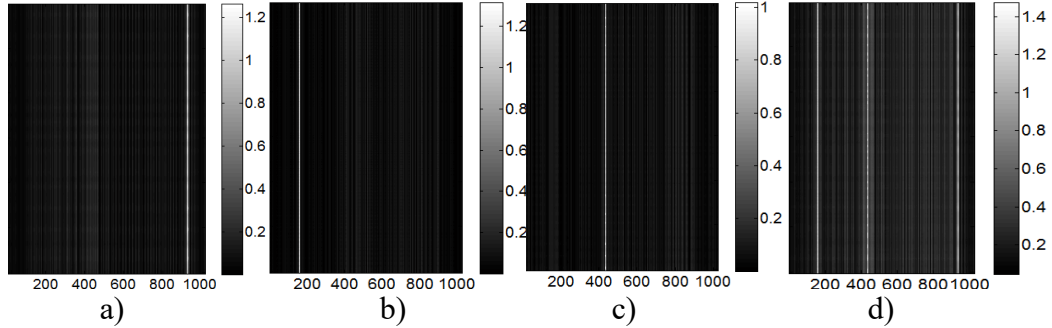


Fig.3. Simulated diffracted foci: (a-c) with displacements depending on wavelengths, and (d) for all wavelengths, at the same distance z .

4. Results

After simulation, the results were achieved in several steps. First, a spatial light modulator (SLM) working in reflection was used to validate the design and to refine the data for label fabrication on polymeric substrate. Second, fabrication parameters were established using dynamic force-temperature analysis. And third, dimensions of the microrelief fabricated in transparent polymers were checked.

4.1 Experimental diffracted intensity pattern

SLM is a liquid crystal-based device which can work in reflection or transmission, depending on the way it is manufactured. Since the structures to be included in the holographic mark would be manufactured on Al foil, here the reflection version was preferred (HoloEye GmbH, reflection type, Pluto HES 6010. 420-810nm, HDTV Developer phase only kit, resolution 1920×1200 , pixel pitch $8.1\mu\text{m}$, filling factor: 90%, electronic driver PCIe16 graphics card). The structures simulated in MATLAB were addressed on the SLM of the two-level, phase only diffractive elements (white meaning Pi phase shift, and black meaning no shift).

The experimental setting includes a tunable He-Ne laser (Research Electro Optics Boulder, Colorado, tunable HeNe laser, model 30603, 4mW, stabilized) working at 543nm, 594nm, and 633nm in line with the simulations, a beam expander (ThorLabs BE-05-10-A) up to the size of the active area of the SLM to get maximum finesse for the diffracted pattern, a reflective SLM, and a high resolution CCD camera (Pike F421C, sensor type 1.2 KODAK KAI-4021, 2048×2048/14bit color, 16fps; transfer rate 100-800 Mb/s, Pentax objective, Interface firewire IEEE1394b for gigabit signals) normal to the propagation axis to record the diffracted intensity pattern.

The analysis of the diffracted intensity distribution recorded by CCD in planes perpendicular to the propagation axis confirms that, for a given wavelength and at designed z distances there is a single sharp focal line together with the remaining part of the beam, given by the position of CFL in the hybrid arrangement (Fig.4 a-c).

To enhance the separation of the focal lines and to better steering the foci positions by wavelength, a hyperfine structure of linear gratings of adequate periods were superposed on each CFL. In Fig.4 d-f are shown the changes of the lateral displacements dependent on the grating period.

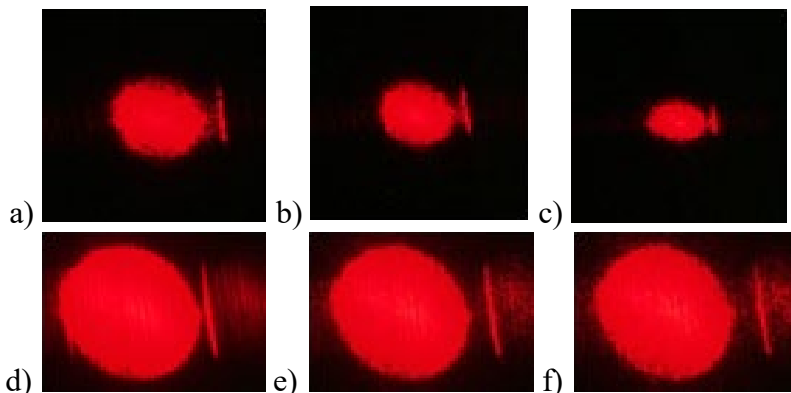


Fig.4 Axial (a-c) and transversal (d-f) control of the focal line positions, $\lambda_3=633\text{nm}$

4.2 Polymer microrelief fabrication

To obtain the ensemble of CFLs superposed with rectilinear gratings, the fabrication processes consist in several conventional steps starting with a mask made in a photoresist layer, then transferred in a Ni shim, the microstructures being hot embossed in transparent polymers with two-phase levels and finally the microrelief is transferred on Al foil.

The photoresist mold was made with the KineMax equipment (Polish Holographic Systems PSH, graphics resolution up to 120000dpi, standard exposing area 200×200mm, positioning control 0.1 μm resolution absolute linear encoders, automatic optoelectronic focusing, mastering speed up to 3 cm^2/hour at resolution

120,000 dpi). It has the possibility to imprint hyperfine structures at different angles or with different network constants. In the present study, we adjusted the grating constants to obtain enough large angles to the reflected beam so that the foci do not overlap.

The polymer used for hot embossing was a poly(3-hydroxybutyrate) in the form of plates of 150mm×150 mm×1.5 mm. Poly(3-hydroxybutyrate) is an aliphatic polyester (PES). For a proper embossing process, a dynamic mechanical analysis using a DMA Q800 from TA Instruments has been undertaken on the polyester plates. Cylindrical samples of 1mm thickness and 10mm diameter were tested in DMA controlled force mode at a heating rate of 3°C/min up to 100°C. In Fig.5 are given the displacement vs. temperature curves for different force values.

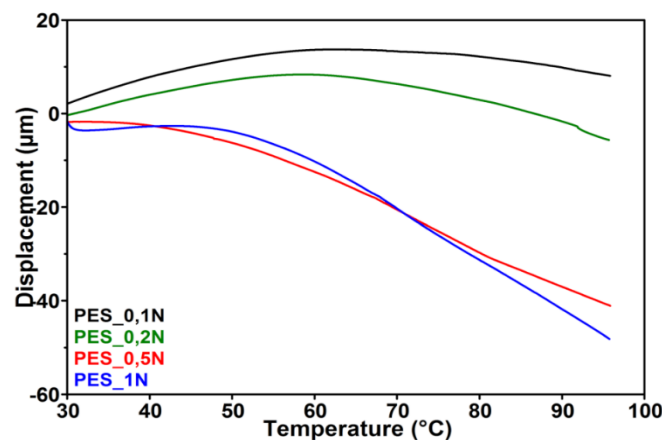


Fig.5. DMA displacement vs. temperature curves for different force values

It can be observed that for the low values of the force (0.1N and 0.2N) the displacement was almost zero regardless of the temperature while for higher force values (0.5N and 1N) the displacement became significant. A displacement of about 30μm was obtained at 80°C, a temperature close to that used for imprinting, for both applied forces, 0.5N and 1N.

4.3 Polymer microrelief characterization

To characterize the microrelief imprinted in polymer, the method of quantitative phase imaging was used (Lynceetec, DHM® T-1000 operating with a single laser, 0.8μm spatial resolution in the transverse plane, 100nm axial resolution). The interferometric configuration of the system allows for recording transparent structures such that to retrieve 3D images and to measure the geometric dimensions (width, peak and depth) of the structures. It is a fast technique, it does not require scanning when acquiring the samples, and it also provides information about the dimensions along the propagation axis.

A detail of the diffraction grating structures of different angles and periods is shown in Figs.6a-c. A 3D image is in Fig.6d where the color bar was calibrated in nanometers, assuming a refractive index of the PES $n_{PES}=1.5$ [10]. On profiles of the type shown in Fig.6e one can measure the constant of the hyperfine gratings and their depths as well.

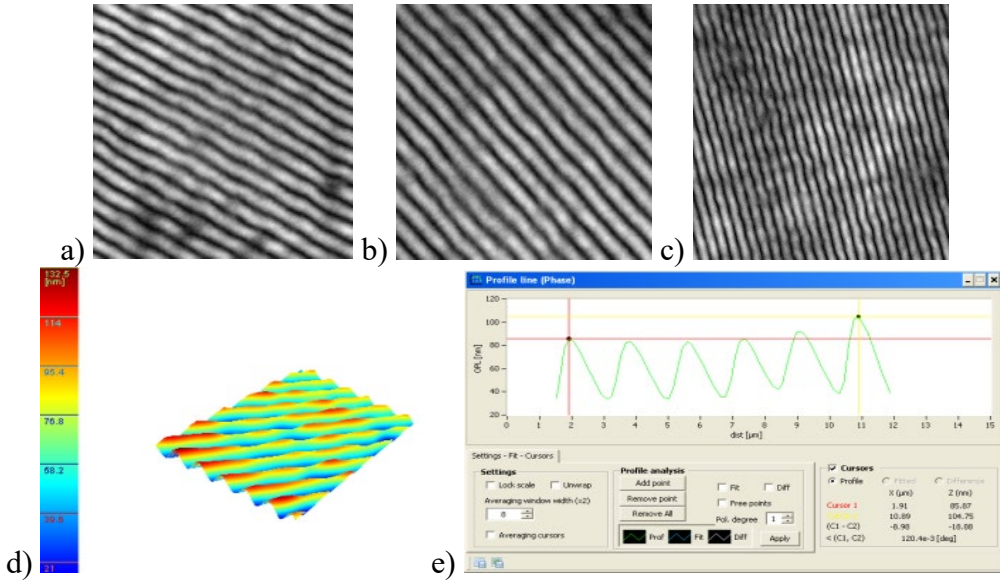


Fig.6 Microrelief characterization: a)-c) quantitative phase images of microreliefs at different angles and periods, d) retrieved 3D microrelief, and e) profile analyzer.

In Fig.7a is an image on a larger area of the CFL microstructures with a detail that highlights the diffraction gratings used for steering. On the profile shown in Fig.7b one can remark the hyperfine structures of the linear grating, with approximately uniform peaks and spatial periods. The measurements on several of the manufactured samples revealed periods between 0.8 and 1.2 μ m and depths of the order of hundreds of nanometers.

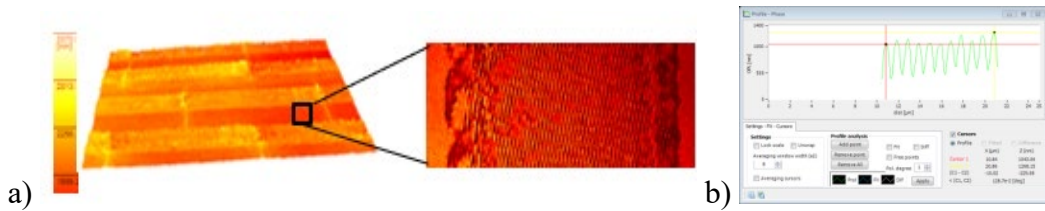


Fig.7. a) Detail of the hyperfine diffraction grating, and b) profile analyzer.

6. Discussions and conclusions

A system of three CFLs is proposed to enhance the security level of the holographic labels. It is designed to steer three different wavelengths and to focus them at equal distances (of the order of a few millimeters) from the diffractive elements in the form of separate bright lines. To increase the separation distances between the focal lines, a hyperfine structure of linear gratings was superposed. The steering control has been done using gratings with adequate periods on each CFL such that the lateral displacements of the focal lines lie in millimeter range in planes perpendicular to the propagation axis.

The diffractive system was designed, implemented, and simulated using MATLAB software. The manufacturing process in a two-phase levels PES polymer has been assisted by DMA. The fabrication was carried out on industrial installations with satisfactory reproducibility and uniformity of the microrelief as revealed by the quantitative phase analyses.

These lead us to hope that this type of security element can be included in the holographic labels for end users.

Acknowledgements

The research presented in this paper is supported by the Romanian Authority for Scientific Research Innovation, contr. UEFISCDI, PN-III-P2-2.1-PTE-2021-0339 No. 78PTE/2022, HOLTERM.

R E F E R E N C E S

- [1] *K. Patorski, K. Pokorski, M. Trusiak, „Circular-linear grating Talbot interferometry with moiré Fresnel imaging for beam collimation”*, Opt. Lett. 39, no. 2, 291, 2014.
- [2] *L. Ionescu, D. Ursescu, L. Neagu, M. Zamfirescu, "On-site holographic interference method for fast surface topology measurements and reconstruction"*, Phys. Scripta, 90, 6, 065502, 2016.
- [3] *X. Meng, E. Drouard, G. Gomard, R. Peretti, A. Fave, C. Seassa, „Combined front and back diffraction gratings for broad band light trapping in thin film solar cell”* Opt. Expr. 20, S5, A560, 2012.
- [4] *X.-F. Li, S. O'Brien, R.J. Winfield, „Absorptive structures fabricated by laser writing”*, J. Optoelectron. Adv. M. vol. 12, iss. 3, 595, 2010.
- [5] *Q. Huang, J. Wang, B. Quan, Q. Zhang, D. Zhang, Li, Meng, Pan, Wang, Yang, Appl. Opt. 52, 11, 2312, 2013.*
- [6] *M. Mihailescu, A. Craciun, R.A. Gabor, C.A. Nicolae, M. Pelteacu, B. Comanescu, G. Bostan, „Diffractive microstructures with twin focal points”*, UPB Sci. Bull., A, vol. 80, Iss. 2, 2018
- [7] *D. C. O'Shea, T. J. Suleski, A. D. Kathman, and D. W. Prather, Diffractive Optics: Design, Fabrication, and Test*, SPIE Press, 2004.
- [8] *J.W. Goodman*, Introduction to Fourier Optics, Mc Graw-Hill Book Company, 1968.
- [9] *M. Mihailescu, A. M. Preda, D. Cojoc, E.I. Scarlat, L. Preda, “Diffraction patterns from a phyllotaxis type arrangement”*, Optics and Lasers in Eng., vol. 46, no. 11, 2008, 802-809.
- [10] *I. Keen, L. Raggatt, S. Cool, V. Nurcombe, P. Fredericks, M. Trau, et al., “Investigations into poly(3-hydroxybutyrate-co-3-hydroxyvalerate) surface properties causing delayed osteoblast growth”*, J. Biomater. Sci. Polym. Edn. Vol 18, 2007, 1101e1123.